Research Highlights

Discovery of models, small molecules & herbals, disease mechanism, targets and tools for lifestyle disease management

Efforts were made to address the issue of lifestyle diseases in a holistic manner. New models of lifestyle diseases were developed (*JPB*). Small molecules and herbals were screened and developed using the new and established models of lifestyle diseases (US9206155B2/Dec8, 2015). Besides this significance of druggable targets having importance in lifestyle diseases was realized (*JLR, JI*). Macrophage inflammation, polarization and its critical determinants were identified as crucial events in lifestyle diseases (CMI, BBA, FRBM). This can help in designing interventions for modulating disease progression. A novel diagnostic tools based on macrophage polarization was also identified (*4242/DEL/2015*). This can help in monitoring disease progression.

Details follow.

1) **Development of hyperlipidemic hamsters model showing time dependent pro-thrombotic changes and modulation by anti-platelet drugs**.

J Physiol Biochem. 2011 Jun;67(2):205-16

The present study was undertaken to assess the chronology of major pathological events associated with high cholesterol (HC) diet and their modulation by anti-platelet drugs. Male Golden Syrian hamsters were fed HC diet up to 90 days. Plasma lipid, glucose and coagulation parameters (commercial kits), platelet activation (whole blood aggregation and static adhesion), endothelial dysfunction (aortic ring vasoreactivity), splenocyte TNF-α, IFN-γ and iNOS mRNA transcripts (RT-PCR), and ferric chloride (time to occlusion) induced thrombosis were monitored at 15, 30, 60, and 90 days after HC feeding and compared with normolipidemic hamsters. A significant increase in plasma lipid levels was observed at 15 days of HC feeding, but other parameters remain unaltered. Enhanced ADP, collagen, and thrombin-induced platelet aggregation, splenocyte TNF-α expression along with endothelial dysfunction were observed from 30 to 90 days of HC feeding. Platelet adhesion on collagen-/fibrinogen-coated surface and IFN-γ expression were augmented only after 60 days, while enhanced iNOS expression, reduction in thrombin time, and potentiation of ferric chloride-induced thrombosis was observed only at 90 days of HC feeding. Thus, pathological changes induced by HC diet depend on the duration and extent of hyperlipidemia. Moreover, hamsters treated with anti-platelet drugs aspirin (5 mg/kg) or clopidogrel (10 mg/kg) along with HC feeding exhibited reduction in platelet activation as well as subsequent changes observed in the above mentioned parameters following HC feeding. Since reduction in TNF-α was associated with reversion in endothelial dysfunction and pro-thrombotic state, the role of platelets is implicated in the pathological changes associated with HC feeding.

2) S007-867: A Novel Anti-thrombotic lead candidate drug

Patent: Chiral 3-aminomethylpiperidine derivative as inhibitors of collagen-induced platelet activation and adhesion.

Inventors: Dikshit DK, Dikshit MD, Irshad T, Siddiqui, Kumar A, Bhatta R, Jain GK, Barthwal MK, Misra A, Khanna V, Prakash P, Jain M, Singh V, Gupta V & Dwivedi AK.

US Patent Granted: US9206155B2/Dec8, 2015

Salient Highlights of the anti-thrombotic molecule:

Antithrombotic drugs are used in the management of clinical conditions like deep vein thrombosis (DVT), pulmonary embolism (PE), peripheral artery disease (PAD), and acute coronary syndromes (ACS). Antithrombotic drugs are one of the most rapidly growing sectors of the cardiovascular market representing >$20 billion USD in sales.

S007-867 is a novel small molecule anti-platelet compound which may be useful in treating intravascular arterial thrombosis. This novel compound (chiral) is patented and has a unique scaffold. The compound was picked after extensive SAR studies, which are active and selectively inhibit collagen-mediated platelet activation. The compound is relatively simple to synthesize (MW < 500) and can easily be chemically modified to obtain the desired ratio of anti-platelet activity.

Unique Features

- First in Class orally effective and reversible inhibitor of collagen-induced platelet adhesion and aggregation
- Has no effect on coagulation parameters viz. Thrombin Time (TT), Prothrombin Time (PT), and activated Partial Thromboplastin Time (aPTT).
- Significantly reduces thrombosis in various experimental models.
- Better than Aspirin, Clopidogrel with minimal bleeding risk in mice at an effective dose of 13mg/kg.
- Does not modulate plasma glucose and lipids level
- More potent than the “gold standard” anti-thrombotic drug, Aspirin, clopidogrel, losartan, EXP3179
- Safety pharmacology, mutagenic and toxicity studies in rodents demonstrate no adverse effect.
- It has been tested *in vitro* for binding to 451 kinases and important GPCRs.
- Good pharmacokinetic profile.
- IND to be filed shortly after Toxicity Studies in a primate model.

Physico-Chemical Properties- Lipinski’s rule compliant

Excellent efficacy in mouse anti-thrombotic animal models:

- Higher efficacy at a lesser dose as compared to standard drugs (Aspirin and Clopidogrel).
- Reduced bleeding risk with better efficacy as compared to Aspirin/ Clopidogrel
- Better efficacy as compared to Aspirin / Clopidogrel.

- Convenient route of administration (oral)
- Blockade of only collagen-mediated activation (Lesion specific) **First in Class**
- Appear to work via a new/specific mechanism
- Target/Cell Specificity will reduce side effects

Pharmacological Profile

- The compound S007-867 effectively and reversibly inhibits collagen-induced platelet aggregation (S007-867 IC_{50}= 6.6µM).
- Used in small doses (13mg/kg), it significantly prevents the incidence of thrombosis in various experimental models (Arterio-venous shunt, Ferric chloride-induced arterial thrombosis, Collagen epinephrine-induced thrombosis).
- It is more potent than the "gold standard" anti-thrombotic drug, Aspirin, clopidogrel, and other collagen inhibitors losartan, EXP3179
- Bleeding time in mice (Far better than Aspirin and Clopidogrel)

Efficacy Profile

Studies	**Results**
Efficacy (in-vivo)	ED 13 mg/kg (mice)
Collagen-epinephrine induced thrombosis in mice	The effect lasts for >24 hrs
Bleeding Time in mice	~1.5 fold
Arterio-venous shunt model in rat	Protective
Arterio-venous shunt model in hyper-lipidemic hamsters	Protective
Ferric chloride-induced thrombosis in rats	Protective
Ferric chloride-induced thrombosis in hyper-lipidemic hamsters	Protective
Inhibition of collagen-induced platelet aggregation studies (Human) IC50	6.6 µM
Inhibition of collagen-induced release reaction, phosphorylation of signaling proteins (Syk, Lyn, Src kinases, PLCγ2) and elevation in intracellular calcium	Effective
Platelet adhesion inhibition (mice and humans)	Effective

Whole blood aggregation inhibition in hyperlipidemic hamsters	Effective
Platelet adhesion inhibition in hyperlipidemic hamsters	Effective
Clot retraction (Human)	Not affected
Preservation of endothelial function in hyperlipidemic hamsters	Effective

Current status: DCGI approval obtained (**Approval no. CT/ND/03/2020**), Phase 1 clinical trial to be initiated

Patent Status

- Indian Patent Filed: 208DEL2011 dated 31-Jan-2011
- European Patent No. 2670722 granted on 12-Oct-2016
- US Patent No. 9206155 granted on 08-Dec-2015
- PCT/IN2011/000032 filed on 12-Jan-2012
- US (div.) 14/933843 filed on 05-Nov- 2015

Advantages of S-007-867

Clinicians have used combination anti-thrombotic drug therapies to improve antithrombotic efficacy. The combined use of antiplatelet agents, however, is considered high-risk by many clinical centers due to increased bleeding tendencies. In addition, the identification of resistance to these drugs is also a matter of great concern. Potent antiplatelet action selectively against collagen-mediated platelet activation offers a novel approach to resolving the bleeding problem. The key advantage of the new compound is related to a novel mechanism of action: Collagen antagonism. Unlike the known anti-platelet drugs, it does not enhance the bleeding time to a very high level as observed with clinically used anti-platelet drugs, thus it is expected to reduce bleeding risks.

3. <u>Critical determinants of macrophage polarization affecting lifestyle diseases.</u>

Innate immune response and macrophages play an important role in lifestyle diseases. A series of studies by Dr. Barthwal's group identifies critical determinants of macrophage polarization that affect the progression of diseases like obesity and heart failure. The concept that M1 macrophages are associated with pro-inflammatory response and M2 macrophages with anti-inflammatory, is oversimplified and a part of Dr. Barthwal's research addresses this point.
Laboratory work demonstrates that in obesity microRNA-99a (miR-99a) plays an important role in tumor necrosis factor (TNF) production and regulates macrophage polarization, obesity, and insulin resistance (*Cell Mol. Immunol. 2021 Sep;18(9):2290-2292 and Cell Mol. Immunol. 2019 May;16(5):495-507.*). At the post-translational level, protein-S-glutathionylation, a reversible phenomenon, promotes redox signaling in physiological and oxidative distress conditions. Galectin-3 (Gal-3) promotes insulin resistance by down-regulating adipocyte insulin signaling,

however, its S-glutathionylation and significance were not known. In a study conducted by Dr. Barthwal's laboratory, M2 macrophages showed enhanced Gal-3 S-glutathionylation when compared to the M1 phenotype. Therefore, M2 macrophage-derived Gal-3 may promote human adipocyte insulin signaling in a glutathionylation-dependent manner. Gal-3 S-glutathionylation is identified as a protective phenomenon associated with M2 macrophage polarization, which relieves Gal-3 inhibitory effect on adipocyte insulin signaling (*Biochim Biophys Acta Mol Cell Res. 2022 Jun;1869(6):119234*).

Therefore, the present study suggests the beneficial role of physiological ROS which may promote insulin sensitivity by promoting Gal-3 S-glutathionylation. This is very different from high levels of ROS which causes irreversibly protein oxidation and loss of function.

More intriguingly, although the loss of ROS generating machinery p47 phox, promotes the abundance of anti-inflammatory M2 macrophage phenotype, a higher degree of cardiac hypertrophy is observed in mice. This study highlights the importance of macrophage p47phox in macrophage polarization and heart failure and suggests that this free radical generating component is very important for limiting M2 phenotype activation and when gone, aggravates cardiac hypertrophy and promotes M2 macrophage polarization (*Free Radic Biol Med. 2021 May 20;168:168-179*). Besides this RNA-binding protein Lin-28B has been known to be a negative regulator for miRNA processing and mature miRNA formation. Work demonstrates role of Lin28B in angiotensin II (Ang-II)-induced Let-7c/miR-99a miRNA formation that consequently affects TNFα production, M1 phenotype activation, and allergic airway inflammation (*Inflammation. 2020 Oct;43(5):1846-1861*.). Therefore, in this study also Let-7c/miR-99a modulates macrophage polarization and disease progression.

Therefore, overall it is observed that critical determinants of miRNA and ROS production regulates macrophage polarization and the progression of lifestyle diseases. Although the physiological and limiting ROS may participate in redox signaling and limited oxidative distress, higher levels may influence disease progression by modulating macrophage inflammation and polarization.

i. **Role of MicroRNA-99a in macrophage polarization, inflammation, and insulin resistance**

Cell Mol Immunol. 2021 Sep;18(9):2290-2292 and Cell Mol Immunol. 2019 May;16(5):495-507.

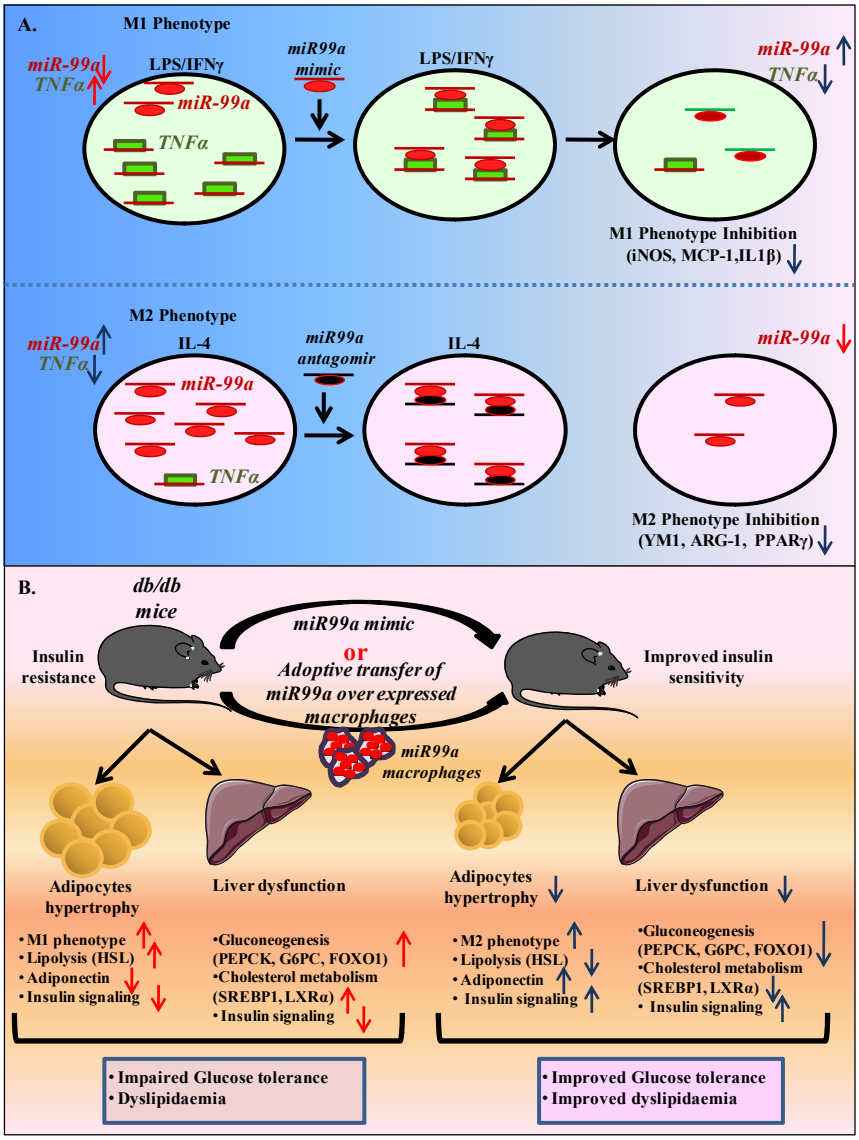

Figure 1. miR99a regulation in macrophage phenotype activation and insulin resistance. **(A)** Effect of miR99a mimic and antagomir on macrophage phenotype **(B)** Effect of miR99a mimic and miR99a over-expressed macrophages on insulin resistance in diabetic *(db/db)* mice. LPS, Lipopolysaccharide; IFNγ, Interferon gamma; IL-4, Interleukin-4; iNOS, Inducible Nitric Oxide Synthase; TNFα, Tumour Necrosis Factor α; MCP, Monocyte chemoattractant protein-1; IL1-β, Interleukin 1 beta; YM1, PPARγ, Peroxisome proliferator-activated receptors gamma; HSL, Hormone Sensitive Lipase; PEPCK, Phosphoenolpyruvate Carboxykinase; G6PK, Glucose-6-phosphatase; FOXO1, Forkhead box protein O1; SREBP1, Sterol regulatory element-binding transcription factor 1, LXRα, Liver X receptor alpha.

In human adipose tissue and obesity, miR-99a expression is negatively correlated with inflammation. Therefore, the present study investigated the role of miR-99a in macrophage phenotype activation and adipose tissue inflammation. M2 BMDMs showed a significant increase in miR-99a expression when compared to the M0 and M1 phenotypes. Phenotype-switching experiments established an association between upregulated miR-99a expression and the M2 phenotype. Overexpression of miR-99a prevented M1 phenotype activation and attenuated bactericidal activity. Likewise, the knockdown of miR-99a abolished M2 phenotype activation. By means of in silico target prediction tools and a luciferase reporter assay, TNFα was identified as a direct target of miR-99a. Knockdown of TNFα recapitulated the effect of miR-99a overexpression in M1 BMDMs. In a db/db mice model, miR-99a expression was reduced in eWAT and F4/80+ ATMs. Systemic overexpression of miR-99a in db/db mice attenuated adipocyte hypertrophy with

increased CD301 and reduced CD86 immunostaining. Flow cytometry analysis also showed an increased M2 and a reduced M1 macrophage population. Mimics of miR-99a also improved the diabetic dyslipidemia and insulin signaling in eWAT and liver, with an attenuated expression of gluconeogenesis and cholesterol metabolism genes in the liver. Furthermore, adoptive transfer of miR-99a-overexpressing macrophages in the db/db mice recapitulated in vivo miR-99a mimic effects with increased M2 and reduced M1 macrophage populations and improved systemic glucose, insulin sensitivity, and insulin signaling in the eWAT and liver. The present study demonstrates that miR-99a mimics can regulate macrophage M1 phenotype activation by targeting TNFα. miR-99a therapeutics in diabetic mice reduces adipose tissue inflammation and improve insulin sensitivity.

ii. **Galectin-3 glutathionylation, macrophage polarization and insulin sensitivity**

Biochim Biophys Acta Mol Cell Res. 2022 Jun;1869(6):119234

Macrophages are phagocytic cells, playing an important role in inflammation, and the generation of ROS, thus regulating diverse processes. S-glutathionylation is a post-translational modification that involves the addition of GSH to protein cysteine thiols. Under oxidative stress conditions, S-glutathionylation of proteins can prevent proteolysis and irreversible oxidation of cysteine residues present in a protein. The ratio of GSH/GSSG decides the redox status of the cell. Galectin-3 (Gal-3) is known to play a role in adipocyte insulin signaling but its oxidative modification and glutathionylation is not known. The present study investigates the importance of macrophage Gal-3 S-glutathionylation and its importance in insulin resistance. The present study suggests Gal-3 S-glutathionylation as a new therapeutic approach for the modulation of metabolic disease.

Gal-3 S-glutathionylation was increased in both murine and human M2 macrophages when compared to M1 macrophages. Bioinformatics analysis showed Gal-3 Cys187 as the putative site which undergoes S-glutathionylation. GSSG treated Gal-3 and GSH+H_2O_2 treated Gal-3 showed enhanced Gal-3 S-glutathionylation compared to native recombinant Gal-3. Mutation of Cys187 to Ser187 mitigates Gal-3 S-glutathionylation, which confirms the specificity of Cys187 S-glutathionylation.

Previously Gal-3 was shown to induce insulin resistance. In the present study, synthesized, recombinant Gal-3 treatment in mature adipocytes results in mitigation of insulin signaling as assessed by insulin stimulated phosphorylation of IRS1 and AKT. Gal-3 treatment also decreases Glut 4 protein expression. However, S-glutathionylation of Gal-3 significantly improves the insulin stimulated phosphorylation of IRS1 and AKT compared to non-glutathionylated Gal-3WT.

To further explore the importance of Gal-3 Cys187 glutathionylation, insulin signaling was evaluated using Cys187 mutant Gal-3 (Gal-3C187S). Treatment of Gal-3C187S decreases insulin signaling just like native Gal-3 WT. Further, GSSG-treated Gal-3C187S does not significantly affect insulin signaling as assessed by insulin stimulated phosphorylation of IRS1 and AKT and the effect

was the same as Gal-3C187S. Above all this, glucose uptake was also studied in 3T3-L1 adipocytes.

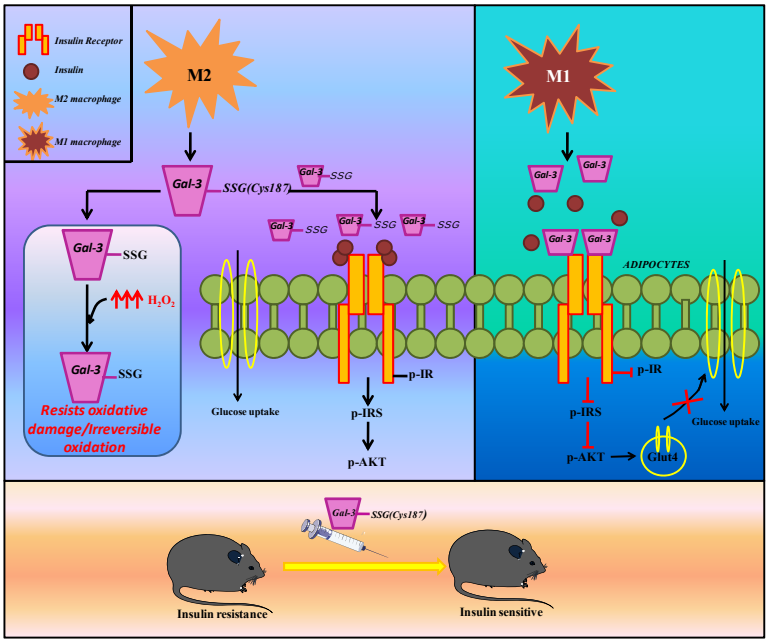

Figure 2: Graphical Illustration Demonstrating the Effect of Gal-3 WT and glutathionylatedGal-3 on adipocytes insulin signaling & its implication in T2DM

Glucose uptake was significantly increased upon insulin treatment compared to untreated/control adipocytes. However, Gal-3WT treatment significantly decreases insulin-stimulated glucose uptake when compared to insulin-treated adipocytes. Interestingly, glutathionylated Gal-3 (GSSG+Gal-3) significantly improves glucose uptake as compared to Gal-3WT. The effect of Gal-3C187S and GSSG+Gal-3C187S on glucose uptake was similar to native Gal-3WT.

To further study the mechanism by which Gal-3WT, GSSG+Gal-3 (Glutathionylated Gal-3), Gal-3C187S, and GSSG+Gal-3C187S affect insulin signaling, an interaction study was performed. Increased interaction was observed between IR and Gal-3WT, Gal-3C187S, and GSSG+Gal-3C187S, compared to Glutathionylated Gal-3 (Gal-3+GSSG). ROS plays an important role in mediating and mitigating glutathionylation**.** So, to assess the extent of Gal-3 S-glutathionylation, Gal-3 was treated with different concentrations of H_2O_2 (0.5µM to 5000µM). In our cell-free system, H_2O_2 is used as an oxidizing agent and GSSG as an S-glutathionylation agent. Up to the concentration of 5µM of H_2O_2, Gal-3 S-glutathionylation gets increased compared to native Gal-3, but, further increasing H_2O_2 concentration (>5µM) Gal-3 S-glutathionylation starts decreasing compared to GSSG+H_2O_2 (5µM) treated Gal-3. S-glutathionylation of Gal-3 protects the protein from irreversible oxidation. As treatment of 500µM H_2O_2 to pre-glutathionylated Gal-3 protects the protein from irreversible oxidation.

Gal-3 is reported to be highly expressed in macrophages. M1 macrophages are considered as oxidative macrophages while M2 macrophage phenotype is characterized as the reductive phenotype. When pathological condition prevails, redox balance gets disturbed and shifts to oxidizing state. Although we did observe endogenous Gal-3 S-glutathionylation in both macrophage phenotypes, surprisingly Gal-3 S–glutathionylation was significantly more in M2 when compared to M1 phenotype, in both BMDMs and HMDMs. Likewise, the secreted Gal-3 was also significantly increased in M2 macrophage phenotype compared to M1 phenotype, in both, BMDMs and in HMDMs. S-glutathionylation of Gal-3 in M2 macrophage phenotype was also confirmed by MALDI-TOF, with a significant score of 57. Protein sequence coverage was 33%. Further, MALDI-TOF also confirms Cys187 as the putative residue in the peptide sequence RVIVCNTK, undergoing S-glutathionylation with a mass increase of 305.

Diabetic patients also show decreased Gal-3 S-glutathionylation compared to a healthy individual. Metformin-treated diabetic mice improve glucose intolerance and decrease the area under the curve compared to saline treated diabetic (*db/db)* mice. Moreover, Metformin treated diabetic (*db/db)* mice significantly increases the S-glutathionylation of Gal-3 compared to saline treated diabetic (*db/db)* mice.
Therefore, this study demonstrated the role of glutathionylated Gal-3 in the regulation of adipocyte insulin signaling and speculates the therapeutic potential of glutathionylated Gal-3 in diabetes

iii. **Role of macrophage p47 phox in polarization and pressure overload-induced left ventricular remodeling**.

Free Radic Biol Med. 2021 May 20; 168:168-179.

It is well known that obesity is associated with RAS activation and obese individual develop diastolic dysfunction. Importantly, our study also found that a high-fat diet regimen in mice for 20 weeks showed a mild increase in circulating Angiotensin II levels in comparison with low-fat diet-fed mice (*p=0.06*, LFD vs. HFD). Therefore, further studies were carried out using the Angiotensin II infusion mice model to develop diastolic dysfunction. NADPH oxidase (Nox) mediates ROS production and contributes to cardiac remodeling. However, macrophage p47phox, a Nox subunit regulating cardiac remodelling, is unclear. We aimed to investigate the role of macrophage p47phox in hypertensive cardiac remodeling and also assess macrophage polarization.
Angiotensin infusion in $p47^{phox}$ knockout (KO) mice showed aggravated cardiac remodelling in comparison with WT Angiotensin II-infused mice, as established from the results that the loss of endogenous $p47^{phox}$ leads to severe cardiac hypertrophy and an obvious deterioration in diastolic heart function. This can be further evinced from excessive altered cardiac biometrics, increased gravimetric ratios (HW/BW and HW/TL), increased cardiomyocyte cross-sectional area, elevated systolic blood pressure, and upregulated fetal cardiac gene transcripts. Moreover, loss of $p47^{phox}$ also led to increased immune cell infiltration which was found to be $CD45^{+}$ and $Mac3^{+}$. Moreover, the infiltrated cells were also found to be locally proliferating as indicated from $ki67^{+}$ labelling. Interestingly, hypertensive $p47^{phox}$ KO mice showed an increased tendency towards an anti-inflammatory milieu as demonstrated by increased M2/anti-inflammatory gene markers and

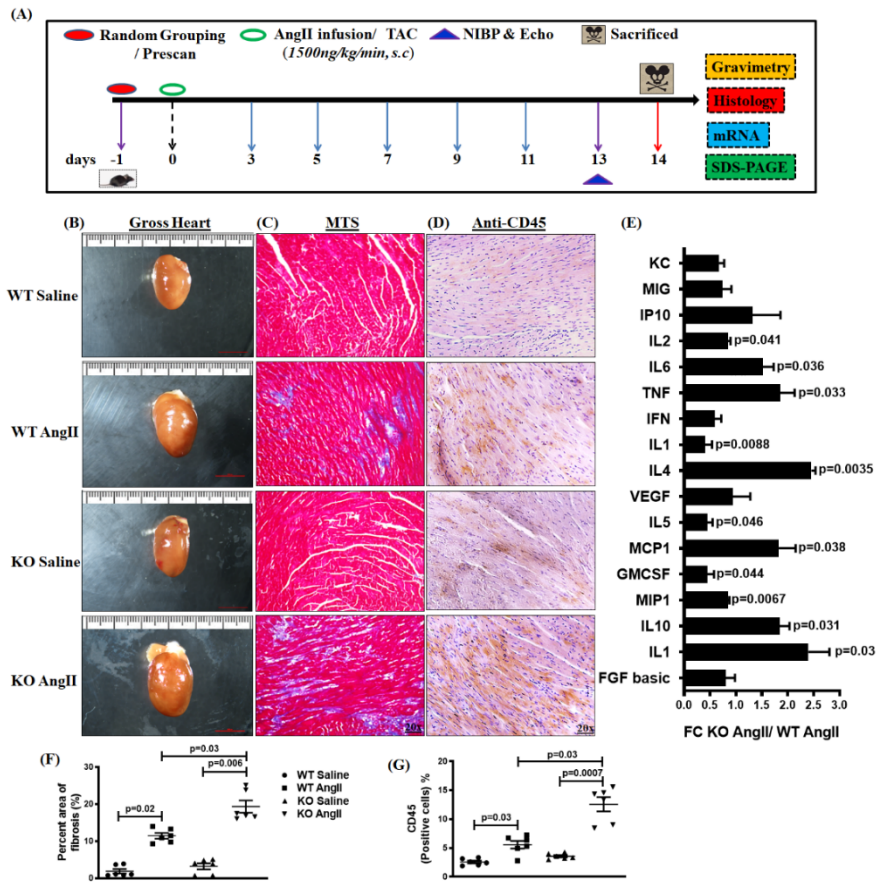

Figure 3: Angiotensin II infusion in p47^{phox} KO mice is associated with enhanced cardiac remodeling**.** (A) Schematic representation of work plan. (B) Heart gross morphology. (C) Masson Trichome staining (MTS) of the LV. (D) Immunohistochemistry of CD45 in the LV. (E) Immunokines multiplexing. (F-G) Quantification of representative images as shown in panel (C) and (D). Data were expressed as mean ± SEM, n= at least 5 per group (except E, n= >10 per group). Total magnification X200. Scale bar 50 µm. FC: fold change.

CD206^{+} cells in the left ventricle region. In addition, hypertensive p47^{phox} KO mice showed accelerated interstitial fibrotic deposition which were majorly found to be thick collagen fibres (type I) and upregulated pro-fibrotic gene transcripts. Subsequently, p47^{phox} KO mice also displayed increased α-sma^{+} cells indicating myofibroblast formation. Furthermore, another model of pressure overload was also applied to show the importance of p47^{phox} in mediating cardiac remodelling. Based on the above findings that AngII-infused KO mice show altered cardiac biometrics and extracellular matrix remodeling, circulating levels of various immunogens were also investigated. Remarkably, AngII-infused KO mice showed prominent changes in the systemic levels of TH1/TH2 related cytokines and chemokines compared to AngII-infused WT mice. Comparably, thoracic aortic constriction (TAC) in p47^{phox} mice showed similar results in line with the AngII infusion model. Besides, AngII-infused p47^{phox} KO mice also showed elevated circulating IL-4 levels. To further substantiate the *in vivo* findings, both AngII and Il-4 stimulation was given in the isolated BMDM's. Importantly, both AngII and IL-4 stimulated p47^{phox} KO macrophages showed upregulated anti-inflammatory macrophage and fibrotic gene markers in comparison with both AngII and IL-4 stimulated WT macrophages.

We next observed the modifications in STAT6 protein phosphorylation (Y641) indicating STAT6 activation. Interestingly, both AngII and IL-4 stimulated KO macrophages showed highly upregulated p-STAT6 protein expression (Y641) compared to both AngII and IL-4 stimulated WT macrophages. To demonstrate the importance of macrophage p47^{phox} in myocardial remodelling, bone marrow transplantation of WT bone marrow into p47^{phox} KO mice (WT to KO) and vice versa

(KO to WT) was performed, followed by AngII infusion for 2 weeks. Therefore, the macrophage-specific deficiency of p47^{phox} was enough to aggregate AngII induced cardiac hypertrophy and fibrosis in mice.

It is well recognized that IL-4 stimulated M2 macrophage polarization is regulated by several transcription factors, such as PPARs and STATs. Therefore, the alterations in IL4/STAT6/PPARγ pathway and SOCS3, a negative modulator of JAK/STAT axis was studied in the LV hypertensive remodelling. Interestingly, AngII-infused KO mice showed significantly upregulated mRNA transcripts of IL-4, PPARγ, SOCS3 and KLF4 compared to AngII-infused WT mice. Likewise, Notably, AngII-infused KO mice showed prominent changes in the p-STAT3, p-STAT6, PPARγ, and SOCS3 protein expression compared to AngII-infused WT mice. To further corroborate the data associated with anti-inflammatory signalling, we also observed the changes in IRF4, OPN1 and KLF4 protein expression. Markedly, AngII-infused KO mice showed prominent changes in protein expression of IRF4, OPN1 and KLF4 compared to AngII-infused WT mice. In line with the AngII data, we also found that both TAC-induced WT and KO mice showed similar alterations in anti-inflammatory signalling. Overall, our studies show that macrophage p47^{phox} limits anti-inflammatory signalling and ECM remodelling in response to pressure overload. These findings suggest possible therapeutic implications for LVH and failure in hypertensive patients.

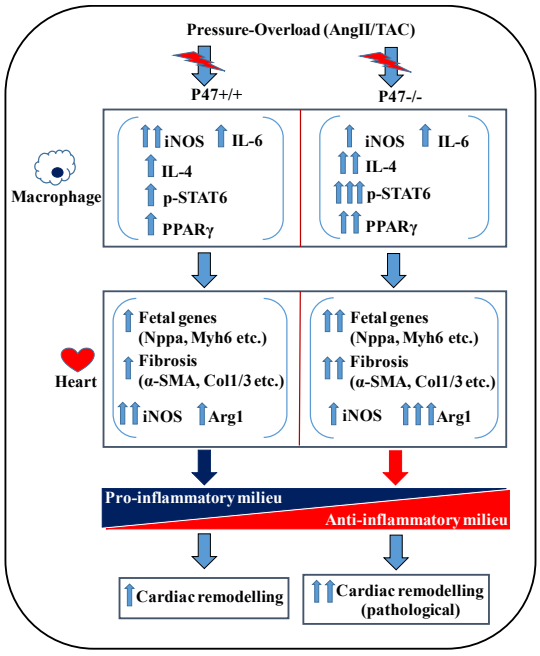

Figure 4: Pathway summary and highlights

1.Pressure-overload in p47phox$^{-/-}$ mice is associated with augmented cardiac hypertrophic and pro-fibrotic response.

2.AngII-infused p47phox$^{-/-}$ mice is associated with altered pro- and anti-inflammatory balance in the left ventricle.

3.AngII and IL-4 treated p47phox$^{-/-}$ macrophages show augmented STAT6 phosphorylation (Y641).

4.Macrophage p47phox plays a crucial role in hypertensive cardiac remodeling in mice.

5.Loss of p47phox is associated with enhanced IL-4/STAT6/PPARγ signaling and downregulated SOCS3 expression in the left ventricle of AngII-infused mice.

iv. **<u>Lin28B regulates Angiotensin II-mediated Let-7c/miR-99a MicroRNA formation consequently affecting macrophage polarization and allergic Inflammation</u>**.

Inflammation. 2020 Oct;43(5):1846-1861.

Angiotensin-II (Ang-II) receptor plays a role in allergic airway inflammation; however, the underlying mechanism and role of macrophages need a better understanding. In the present study, angiotensin-II infusion (1 µg/kg/min) in an ovalbumin-induced airway inflammation mouse model significantly decreased immune cell infiltration, goblet cell hyperplasia, and eosinophil numbers in the lungs. Ang-II infusion increased M1 and decreased M2 macrophage population in bronchoalveolar lavage fluid and respective macrophage markers in lung macrophages. Similarly, in vitro Ang-II treatment in murine bone marrow-derived macrophages (BMDMs) induced M1 and reduced M2 macrophage phenotype with enhanced bactericidal activity. Mechanistically, Ang-II inhibits Let-7c and miR-99a expression in BMDMs and in vivo as well. Lentiviral overexpression of Let-7c and miR-99a miRNAs in BMDMs abrogated Ang-II-induced M1 phenotype activation and promoted M2 phenotype, which is governed by targeting TNFα by miR-99a. In lung macrophages, ovalbumin-induced TNFα inhibition was rescued after Ang-II treatment. In BMDMs, knockdown of TNFα abrogated Ang-II-induced M2 to M1 macrophage phenotype switch and associated bactericidal activity.

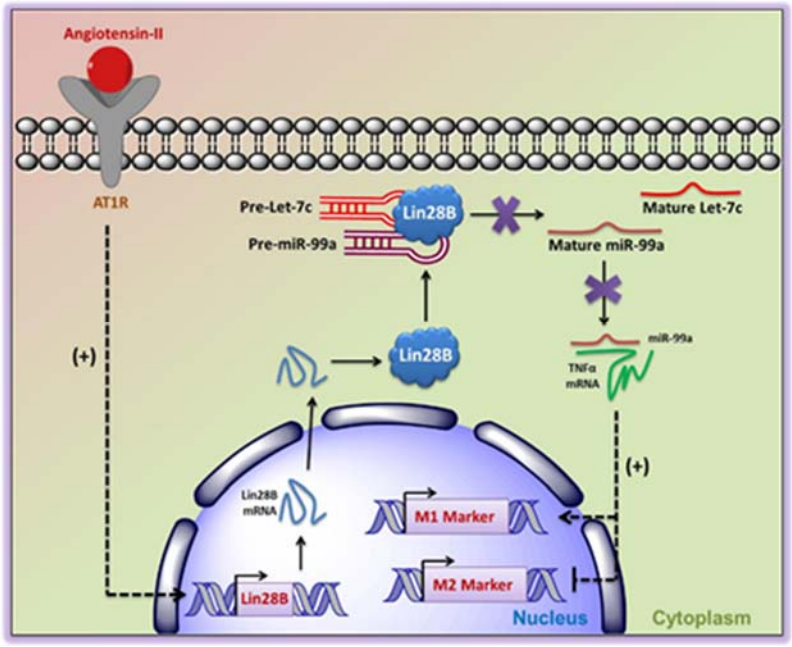

Figure 5. Graphical Illustration Representing the miRNA Mediated Mechanism of Angiotensin-II Induced switch from M2 to M1 macrophage Phenotype Activation.

Ang-II affects mature miRNA formation by enhancing Lin28B levels in macrophages in vivo and in vitro. Furthermore, Lin28B knockdown prevented Ang-II-mediated inhibition of mature Let-7c/miR-99a miRNA formation, M2 to M1 macrophage phenotype switch, and increased bactericidal activity. Therefore, the present study suggests a role of Lin28B in Ang-II-induced Let-7c/miR-99a miRNA formation that consequently affects TNFα production, M1 phenotype activation, and allergic airway inflammation. Graphical Abstract Ovalbumin inhibits LIN28B expression and thereby fails to inhibit premature to mature Let-7c/miR-99a miRNA formation. Mature miR-99a miRNA that inhibits TNFα consequently promotes M2 polarization and allergic airway inflammation. While Ang-II induces Lin28B, which inhibits Let-7c/miR-99a miRNA processing and mature miRNA formation, this results in increased TNFα levels that lead to M1 polarization and allergic airway inflammation inhibition.

4. <u>Role of Interleukin 1 receptor-associated kinase (IRAK) in lipid-induced inflammation, foam cell formation and atherosclerosis: A druggable target for inflammatory and related cardiovascular diseases</u>

J Lipid Res. 2014 Jul;55(7):1226-44, J Immunol. 187:2632,2011, J Lipid Res. 2020 Mar;61(3):351-364., Bioessays. 2016 Jul;38(7):591-604, Arterioscler Thromb Vasc Biol. 2015 Jun;35(6):1445-55.

This study examined the role of interleukin (IL)-1 receptor-associated kinase (IRAK) and protein kinase C (PKC) in oxidized LDL (Ox-LDL)-induced monocyte IL-1β production. In THP1 cells, Ox-LDL induced time-dependent secretory IL-1β and IRAK1 activity; IRAK4, IRAK3, and CD36 protein expression; PKCδ-JNK1 phosphorylation; and AP-1 activation. In addition to this PMA treatment to THP1 cells induced CD11b, TLR2, TLR4, CD36, IRAK1, IRAK3, and IRAK4 expression, IRAK1 kinase activity, PKCδ and JNK phosphorylation, AP-1, and NF-κB activation, and secretory IL-1β production. IRAK1/4 siRNA and inhibitor (INH)-attenuated Ox-LDL and PMA induced secreted IL-1β and pro-IL-1β mRNA and pro-IL-1β and mature IL-1β protein expression, respectively. Diphenyleneiodonium chloride (NADPH oxidase INH) and N-acetylcysteine (free radical scavenger) attenuated Ox-LDL-induced reactive oxygen species generation, caspase-1 activity, and pro-IL-1β and mature IL-1β expression. In PKCδ wild-type overexpressing THP1 cells, IRAK1 kinase activity and IL-1β production were significantly augmented, whereas recombinant inactive PKCδ and PKCδ small interfering RNA significantly inhibited basal and PMA-induced IRAK1 activation and IL-1β production. Ox-LDL-induced secretory IL-1β production was abrogated in the presence of JNK INH II, Tanshinone IIa, Ro-31-8220, Go6976, Rottlerin, and PKCδ siRNA. PKCδ siRNA attenuated the Ox-LDL-induced increase in IRAK1 kinase activity, JNK1 phosphorylation, and AP-1 activation. In THP1 macrophages, CD36, toll-like receptor (TLR)2, TLR4, TLR6, and PKCδ siRNA prevented Ox-LDL-induced PKCδ and IRAK1 activation and IL-1β production.

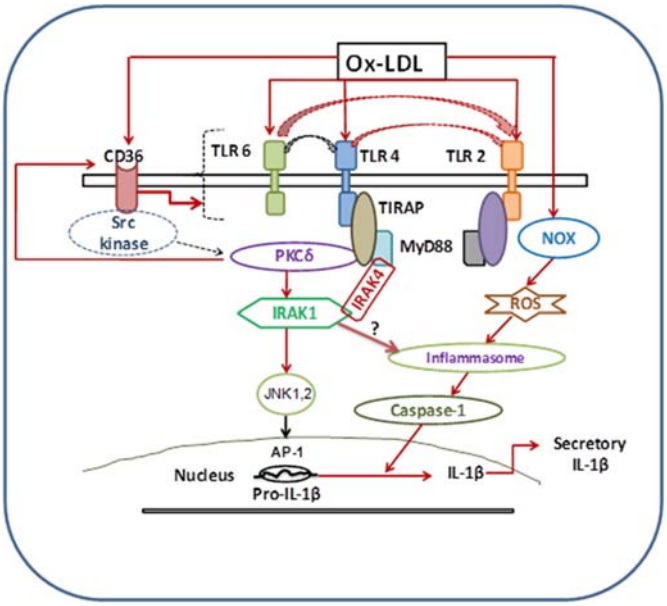

Figure 6: Schematic diagram for Ox-LDL induced IL-1β production in monocytes. Schematic signaling flow diagram integrating reported and presently studied Ox-LDL signaling. Ox-LDL involves CD36, TLR2, 4, 6 for PKCδ-IRAK1-JNK-AP-1 axis activation and IL-1β production. ROS generated after Ox-LDL treatment induces caspase-1 activation and IL-1β processing. PKCδ positively regulates CD36. Ox-LDL induced PKCδ activation can be mediated by CD36, CD36 dependent TLR dimerization, TLR up-regulation, TIRAP or Src activation.

Enhanced Ox-LDL and IL-1β in systemic inflammatory response syndrome (SIRS) patient plasma demonstrated a positive correlation with each other and with disease severity scores. Ox-LDL-containing plasma induced PKCδ and IRAK1 phosphorylation and IL-1β production in a CD36-, TLR2-, TLR4-, and TLR6-dependent manner in primary human monocytes. Results suggest the

involvement of CD36, TLR2, TLR4, TLR6, and the PKCδ-IRAK1-JNK1-AP-1 axis in Ox-LDL-induced IL-1β production.

Besides this role of IRAK was also demonstrated in macrophage foam cell formation (*Bioessays. 2016 Jul;38(7):591-604*) and neo-intimal hyperplasia (*Arterioscler Thromb Vasc Biol. 2015 Jun;35(6):1445-55.*) indicating that it can act as a double edge sword to regulate both inflammation and atherosclerosis, the main pathways involved in the progression of atherosclerotic cardiovascular diseases. Besides this PKM2 was identified as the important metabolic enzyme that can regulate macrophage foam cell formation by striking a balance between oxidative phosphorylation and glycolysis (*J Lipid Res. 2020 Mar;61(3):351-364.*)

5. Identification of Novel Macrophage Phenotype Specific Fluorescent Chemical Probes

Patent: Pyranone fused Aza-heterocyclic fluorescent dyes are useful fluorescent probes.

Inventors: Goel A, Raghuvanshi A, Jha AK, Dogra S, Yadav PN, Jaiswal A, Barthwal MK, 23/Dec/2015, 4242/DEL/2015.

Macrophages are a heterogeneous population of innate immune cells involved in health and disease. They are the most functionally diverse (plastic) cells of the hematopoietic system, found in all tissues, and their main function is to respond to pathogens and to modulate the adaptive immune response through antigen processing and presentation. These macrophages undergo a specific differentiation pattern, depending upon the local tissue environment. Two distinct states of polarized macrophages have been defined, classically activated (M1) macrophage and alternatively activated (M2) macrophage phenotype. M1 macrophages have the role of effector cells in Th1 immune response which shows increase inflammatory as well as anti-microbial property. While M2 macrophages appear to be involved in tissue repair and anti-inflammatory activity. Imbalance in these phenotypes results in progression of several diseases such as Atherosclerosis, Insulin Resistance, aneurysm, Cancer and others.

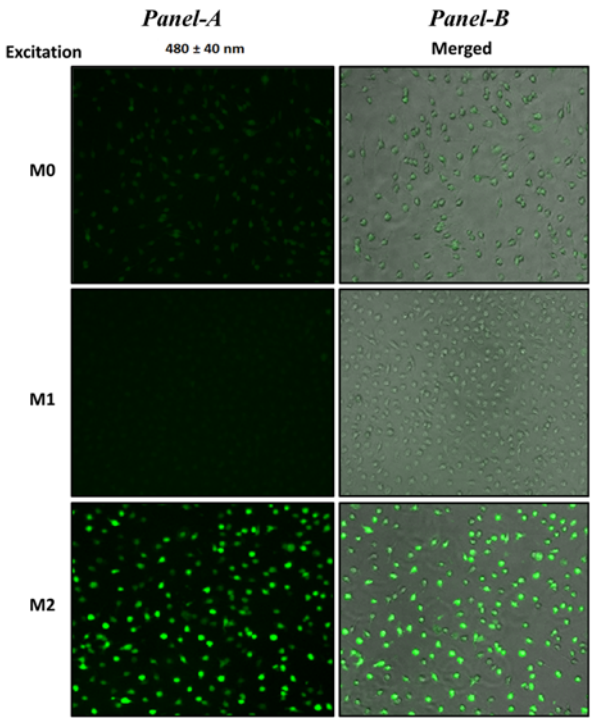

Figure 7: Selective labelling of compound **S-012-0411** in M0, M1 & M2 phenotype. **Panel A** - shows binding fluorescence to the phenotype, **Panel B-** Represents an overlay of phase-contrast & fluorescence image of cells.

To address the role of any small molecule fluorescent probes in phenotype-specific physiological responses, we screened six fluorescent-based compounds to discover novel macrophage cell-permeable fluorescent probes with the ability to label and image live-specific macrophage phenotypes. In this study, we demonstrate that one compound (**S-012-0411**) out of six, selectively stains M2 phenotype, very less for M0 (which resembles slightly to M2 phenotype), but not the M1 phenotypes, which can be applied for multiple imaging on a cellular platform of macrophage phenotype. MCSF differentiated murine bone marrow-derived macrophages were polarized to M1 (10U/ml IFN-γ+1µg/ml LPS) and M2 (10ng/ml IL-4) phenotype or only MCSF as control M0 phenotype. Cells were treated with a 10µM compound and directly observed under a fluorescent microscope (Leica DMI6000 system) after 6hr. The fluorescence of compounds was measured using the filter with an excitation range at 480±40nm and emission at 527±30nm.

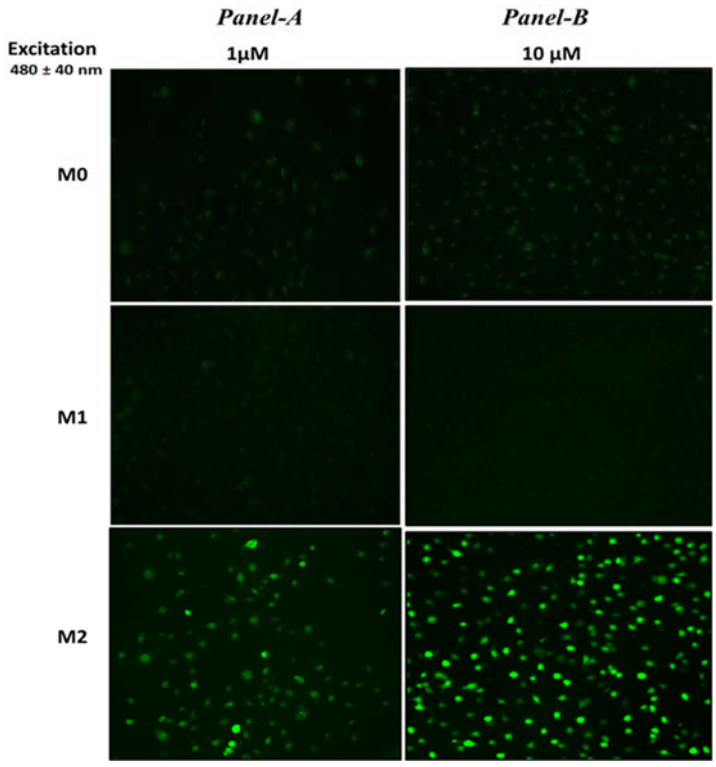

Figure 8: Selective labelling of compound **S-012-0411**at different concentrations in M0, M1 & M2 phenotype. **Panel–A** shows binding fluorescence to the phenotype at 1µm, and **Panel B** depicts fluorescence at10µm concentration.

Six compounds were screened on this macrophage phenotype cell system (M0, M1 & M2 macrophage) to determine if any compound showed phenotype selectivity. We observed that one compound S-012-0411 out of six, specifically labeled the M2 phenotype in a dose-dependent manner at 1µM & 10µM concentrations. Very less labeling was observed in M0 (phenotype having some resemblance to M2), but no labeling was observed in the M1 macrophage phenotype (Figures 7 & 8). While the other five compounds did not show any specificity to these macrophage phenotypes. Therefore, studies led to the identification of compounds specific to the M2 macrophage polarization phenotype which have great application as diagnostic probes in various disorders from obesity to cancer.

6. <u>Hypolipidaemic and anti-inflammatory potential of natural product curcuma oil</u>:

Journal of Functional Foods 2015, (16), 152-163., Br J Nutr. 2013 Aug 28;110(3):437-46.

Essential oil components from turmeric (Curcuma longa L.) are documented for neuroprotective, anti-cancer, anti-thrombotic and antioxidant effects. The present study aimed to investigate the disease-modifying potential of curcuma oil (C. oil), a lipophilic component from C. longa L., in hyperlipidaemic hamsters. Male golden Syrian hamsters were fed a chow or high-cholesterol (HC) and fat-rich diet with or without C. oil (30, 100 and 300 mg/kg) for 28 d. In HC diet-fed hamsters, C. oil significantly reduced plasma total cholesterol, LDL-cholesterol and TAG, and increased HDL-cholesterol when compared with the HC group. Similar group comparisons showed that C. oil treatment reduced hepatic cholesterol and oxidative stress, and improved liver function. Hyperlipidaemia-induced platelet activation, vascular dysfunction and repressed eNOS mRNA expression were restored by the C. oil treatment. Furthermore, aortic cholesterol accumulation and CD68 expression were also reduced in the C. oil-treated group. The effect of C. oil at 300 mg/kg was comparable with the standard drug ezetimibe. Delving into the probable anti-hyperlipidaemic mechanism at the transcript level, the C. oil-treated groups fed the chow and HC diets were compared with the chow diet-fed group. The C. oil treatment significantly increased the hepatic expression of PPARa, LXRa, CYP7A1, ABCA1, ABCG5, ABCG8 and LPL accompanied by reduced SREBP-2 and HMGCR expression. C. oil also enhanced ABCA1, ABCG5 and ABCG8 expression and suppressed NPC1L1 expression in the jejunum. In the present study, C. oil demonstrated an anti-hyperlipidaemic effect and reduced lipid-induced oxidative stress, platelet activation and vascular dysfunction. The anti-hyperlipidaemic effect exhibited by C. oil seems to be mediated

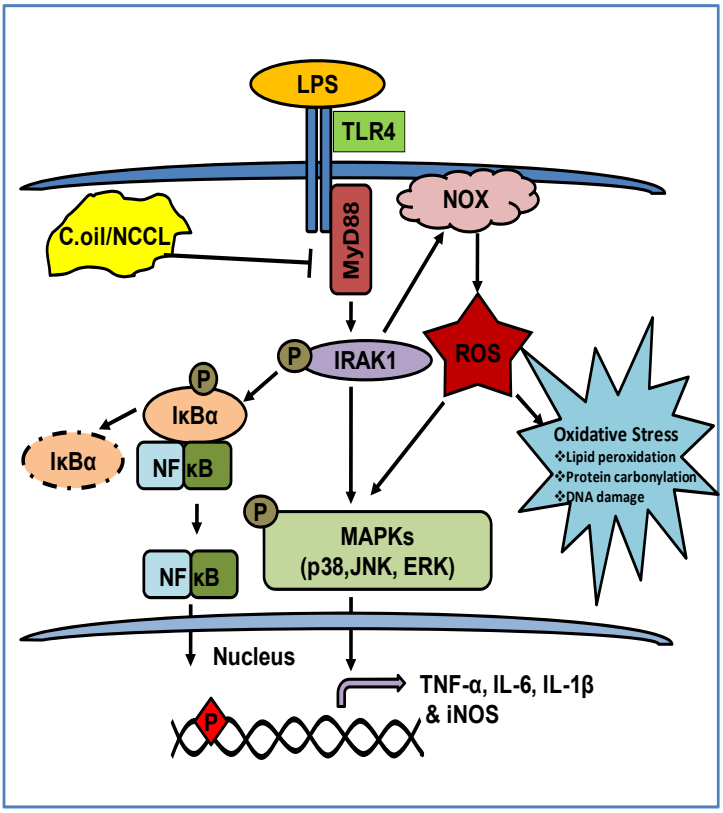

Figure 9. LPS activates TLR4-IRAK1-MAPK-NFκB pathways through TLR4-MyD88 complex formation in the cells. In addition, LPS can also activate MAPKs through ROS. Further, ROS induced oxidative stress *in vivo* leads to proteins, lipids and nucleic acids modification/damage. Phosphorylation of MAPKs induces expression of inflammatory mediators (pro-inflammatory cytokines, iNOS) in LPS stimulated cells. C.oil inhibited TLR4-MyD88 complex formation, IRAK1 and MAPKs phosphorylation and NFκB activation leading to decreased inflammation in the cells

by the modulation of PPARa, LXRa and associated genes involved in lipid metabolism and transport. At the same time anti-inflammatory potential of C.oil was evaluated in the lipopolysaccharide (LPS) induced inflammation in THP-1 human monocytes, J774.2 murine macrophages and Swiss mice. THP-1, J774.2 and mice or human whole blood pre-treated with C.oil (1–30 μg/ml; 14 h) and stimulated with LPS (50 ng/ml–1 μg/ml) showed significant reduction in TNF-α, IL-1β and IL-6 production compared to respective control. C.oil significantly attenuated LPS induced TLR4–MyD88 interaction and IRAK1, MAPK, ROS and NFκB pathway activation in a dose dependent manner. Plasma TNF-α, IL-1β, IL-6, nitrite, aortic iNOS expression and p38 MAPK activation, endothelial dysfunction and oxidative stress markers namely lipid hydroperoxide, 8-hydroxydeoxyguanosine, 8-isoprostane and protein carbonyl were also attenuated in C.oil (100, 300 mg/kg; 10 days p.o.) pre-treated and LPS (10 mg/kg) challenged Swiss mice when compared to LPS alone. The present study gives a mechanistic insight into the nutraceutical potential of C.oil for preventing endotoxin induced inflammatory sepsis.

Therefore *C. oil* demonstrates anti-inflammatory and hypolipidaemic effect.

7.Standardized fraction of *Xylocarpus moluccensis* inhibits inflammation and macrophage polarization by modulating MAPKs, ROS and PKM2 pathway

Inflamm Res. 2022 Apr;71(4):423-437

Present study investigates the effect of Xylocarpus moluccensis (Lamk.) M. Roem fruit fraction (CDR) on endotoxemia and inflammation associated metabolic reprogramming by exploring the underlying mechanisms. The effect of CDR (1-100 μg/ml) was assessed on cytokines, MAPKs, ROS, and metabolic reprogramming in LPS-induced cells (J774.2 and THP-1) by the conventional methodology of ELISA, PCR, and Western blotting. The effect of CDR (1-50 mg/kg, p.o.) was also evaluated in the mice model of endotoxemia and sepsis. CDR prevents LPS-induced cytokine production from murine and human whole blood and cell lines. CDR suppressed total cellular and mitochondrial superoxide generation and preserved mitochondrial function in LPS-stimulated phagocytes. Additionally, CDR abrogated LPS-induced MAPK's phosphorylation and IκBα degradation in J774.2 cells. Moreover, CDR suppressed LPS-induced glycolytic flux as indicated from PKM2, HK-2, PDK-2, and HIF-1α expression in J774.2 cells. In vivo, CDR pre-treatment inhibited pro-inflammatory cytokines release, metabolic reprogramming from oxidative phosphorylation to glycolysis in both LPS-induced endotoxemia and cecal slurry-induced sepsis mice model. CDR exerts its beneficial effect by inhibiting M1 macrophage phenotype and promoting M2 macrophage polarization since it attenuates LPS induced pro-inflammatory genes (IL-6, TNF-α, IL-1β, iNOS) and promotes the anti-inflammatory genes and M2 macrophage-specific markers (IL-4, IL-10, Arginase-1, YM-1). Therefore, present study demonstrates the protective effect of CDR on LPS-induced inflammation and sepsis and identifies MAPK-NFκB and ROS-HIF1α-PKM2 as the putative target axis. Therefore, CDR may exert anti-inflammatory and beneficial effects by modulating macrophage mitochondrial function, aerobic glycolysis, macrophage polarization and inflammation.

References:

1) Jaiswal A, Reddy SS, Maurya M, Maurya P, Barthwal MK. Cell Mol. Immunol. MicroRNA-99a mimics inhibit M1 macrophage phenotype and adipose tissue inflammation by targeting TNFα. 2019 May;16 (5):495-507.
2) Singh A, Singh V, Tiwari RL, Chandra T, Kumar A, Dikshit M, Barthwal MK. The IRAK-ERK-p67phox-Nox-2 axis mediates TLR4, 2-induced ROS production for IL-1β transcription and processing in monocytes. Cell Mol Immunol. 2016 Nov;13(6):745-763.
3) Jain M, Singh A, Singh V, Barthwal MK. Involvement of interleukin-1 receptor-associated kinase-1 in vascular smooth muscle cell proliferation and neointimal formation after rat carotid injury. Arterioscler Thromb Vasc Biol. 2015 Jun;35(6):1445-55.
4) Reddy SS, Agarwal H, Jaiswal A, Jagavelu K, Dikshit M, Barthwal MK. Macrophage p47 phox regulates pressure overload-induced left ventricular remodeling by modulating IL-4/STAT6/PPARγ signalling. Free Radic Biol Med. 2021 May 20;168:168-179.
5) Maurya M, Jaiswal A, Gupta S, Ali W, Gaikwad AN, Dikshit M, Barthwal MK. Galectin-3 S-glutathionylation regulates its effect on adipocyte insulin signaling. Biochim Biophys Acta Mol Cell Res. 2022 Jun;1869(6):119234.
6) Singh V, Rana M, Jain M, Singh N, Naqvi A, Malasoni R, Dwivedi AK, Dikshit M, Barthwal MK. Curcuma oil ameliorates hyperlipidaemia and associated deleterious effects in golden Syrian hamsters. Br J Nutr. 2013 Aug 28;110(3):437-46.
7) Agarwal H, Sukka SR, Singh V, Dikshit M, Barthwal MK. Standardized fraction of Xylocarpus moluccensis inhibits inflammation by modulating MAPK-NFκB and ROS-HIF1α-PKM2 activation. Inflamm Res. 2022 Apr;71(4):423-437.
8) Rana M, Reddy SS, Maurya P, Singh V, Chaturvedi S, Kaur K, Agarwal H, Ahmad H, Naqvi A, Dwivedi AK, Dikshit M, Barthwal MK. Turmerone enriched standardized Curcuma longa extract alleviates LPS induced inflammation and cytokine production by regulating TLR4–IRAK1–ROS–MAPK–NFκB axis. Journal of Functional Foods 2015, (16), 152-163.
9) Gupta P, Kumar A, Pal S, Kumar S, Lahiri A, Kumaravelu J, Chattopadhyay N, Dikshit M, Barthwal MK. Standardized Xylocarpus moluccensis fruit fraction mitigates collagen-induced arthritis in mice by regulating immune response. J Pharm Pharmacol. 2020 Apr;72(4):619-632.
10) Jaiswal A, Maurya M, Maurya P, Barthwal MK. Lin28B Regulates Angiotensin II-Mediated Let-7c/miR-99a MicroRNA Formation Consequently Affecting Macrophage Polarization and Allergic Inflammation. Inflammation. 2020 Oct;43(5):1846-1861.
11) Singh V, Jain M, Prakash P, Misra A, Khanna V, Tiwari RL, Keshari RS, Singh S, Dikshit M, Barthwal MK. A time course study on prothrombotic parameters and their modulation by anti-platelet drugs in hyperlipidemic hamsters. J Physiol Biochem. 2011 Jun;67(2):205-16.
12) Kumar A, Gupta P, Rana M, Chandra T, Dikshit M, Barthwal MK. Role of pyruvate kinase M2 in oxidized LDL-induced macrophage foam cell formation and inflammation. J Lipid Res. 2020 Mar;61(3):351-364
13) Tiwari RL, Singh V, Singh A, Rana M, Verma A, Kothari N, Kohli M, Bogra J, Dikshit M, Barthwal MK. PKCδ-IRAK1 axis regulates oxidized LDL-induced IL-1β production in monocytes. J Lipid Res. 2014 Jul;55(7):1226-44.
14) Tiwari RL, Singh V, Singh A, Barthwal MK. IL-1R-associated kinase-1 mediates protein kinase Cδ-induced IL-1β production in monocytes. J Immunol. 2011 Sep 1;187(5):2632-45.

(Dr Manoj Kumar Barthwal) Date: Aug. 29, 2023.